Journal of Bio- and Tribo-Corrosion (2019) 5:60
https://doi.org/10.1007/s40735-019-0250-8

Microstructure and Corrosion Characteristics of In Situ Aluminum Diboride Metal Matrix Composites

Samuel Dayanand[1] · Satish Babu Boppana[2] · Joel Hemanth[2] · Aravinda Telagu[2]

Received: 13 March 2019 / Revised: 17 April 2019 / Accepted: 3 May 2019 / Published online: 28 May 2019

Abstract
The present work relates to the preparation of Al–AlB_2 in situ composite and investigates the characteristics of corrosion of in situ composites in sodium chloride media. Composites containing matrix alloy, $XAlB_2$ (X—1, 3, and 5 wt%), were prepared by an in situ technique involving the chemical reaction between base matrix and halide salt KBF_4. To know about the uniform distribution of AlB_2 dispersoid in the Al6061 base matrix, microstructural characterization was carried out using SEM. Potentiodynamic Tafel polarization curves have fetched some of the electrochemical parameters. Outcome of the research concludes that higher corrosion resistance was offered by composites compared to base matrix in the selected corrosion media.

Keywords Aluminum diboride · In situ · Corrosion · Stir casting

1 Introduction

Metal Matrix Composites (MMCs) with Aluminum is widely utilized in many diverse usage because of its enhanced properties, for example, quality, sturdiness, hardness, strength-to-weight ratio, rigidness, customized thermal coefficient expansion and thermal conductivity, resistance to corrosion, and so on. Further enhancement of MMCs has been carried out because of the expansion in the quantity of utilizations in Automobile and Aerospace sectors [1, 2]. Aluminum metal matrix composite (AMMC) materials have been created over the most recent years and are possible potential candidates for many applications including marine, airplane skins, ocean vehicles, turbine motors segments, and so forth, because of its novel blends of properties [3–10]. In the present era, composites prepared with in situ technique have achieved additional consideration in the recent years because of clean and transparent interface between the base matrix and the reinforcement, good adhesion strength, greater interfacial virtuousness, and uniform distribution in the base matrix with enhanced attributes and lower cost of composite generation. Different new preparing procedures are being introduced to have superior in situ composites with improved interfacial similarity and diminished reinforcement particle size. Utilizing in situ methods, ultrafine ceramic particles (TiB_2, AlB_2) can be introduced into different materials [11–13]. Very meager amount of work has been carried out on the fabrication in situ Al–AlB_2 composites [14]; however, a few researchers have worked on preparing master alloys (Al–B), for producing in situ AlB_2 particle for strengthening aluminum metal matrix composites [15, 16]. AlB_2 phase possess higher modulus, higher strength, and higher density (3.19 g/cm^3) [17] compared to aluminum in liquid phase (2.4 g/cm^3) at 800 °C. Reinforcement phase of AlB_2 in Al/AlB_2-type composites is formed in situ in the molten aluminum. A homogeneous distribution of reinforcement phase is observed, and hence a phase with perfectly bonded matrix and reinforcement is attained. AlB_2 boride particles appear as thin hexagonal flakes within the matrix [18, 19].

Prior research shows that the microscopic structures of MMCs exposed to cooling at higher rate showed the presence of aluminum diboride particulates in composites [20]. Aluminum diboride is proficiently synthesized and produced

✉ Samuel Dayanand
samueldayanand@gmail.com

✉ Satish Babu Boppana
satishbabu3@yahoo.co.in

[1] Department of Mechanical Engg, Government Engineering College, Raichur, Karnataka, India

[2] Mechanical Engineering, Presidency University, Bangalore, Karnataka, India

by utilization of aluminum-transition high-temperature arrangement in the flux solution. Producing and precipitating AlB_2 particles in the base Al6061 matrix yields us a material procedure to fabricate in situ aluminum diboride composites; however, increasing the effectiveness remains as yet a challenge for producing of AlB_2 particles in the matrix [21].

AMMCs are extensively used in industrial applications, and hence, it is significant to know about the corrosion characteristics of AMMCs [22, 23]. The major disadvantage of the reinforced MMCs is the reinforcement effect on the rate of corrosion since it decreases the protective oxide film in aluminum alloy-based composite [24–26]. Composites are exposed to a number of corrosive environments during the process like cleaning, pickling, and so on. Aluminum materials and their alloys show high rates of corrosion in corrosive media [27–30]. Specifically, severe corrosion is seen in boron–aluminum MMCs when exposed to marine environments, and MMCs are significantly less corrosion resistant compared to unreinforced alloys of aluminum [31, 32]. The aim of this paper was to fabricate Al–AlB_2 composites using in situ method by stir casting processes, and to analyze the corrosion behaviors of composite and of matrix materials in basic media solutions by making use of Tafel polarization curves using potentiodynamic corrosion instrument setup.

2 Experimental Work

2.1 Fabrication and Characterization

In the present research work, 6061Al alloy is used as matrix material to produce in situ composites. The chemical composition of the alloy is given in the Table 1. The composites were prepared by using different compositions (1, 3, and 5 wt%) of halide salt KBF_4. Sodium hexafluoro aluminate (Na_3AlF_6) cryolite is included as a driver for the chemical reaction as explained below.

Al6061-AlB_2 in situ composites with 1, 3, and 5 wt% of aluminum diboride dispersoids were fabricated by the exothermic chemical reaction between Al6061 base matrix and halide salt KBF_4 in an electrical resistance attached with an automatic stirrer and thermocouple. Researchers had realized that a reaction time of 1 h was sufficient for the reaction to be completed; however, a reaction temperature of around 800 °C was required for the formation of hexagonal shape aluminum diboride particles [33]. Hence, the present work was carried out under the same reaction time and temperature to produce in situ composites. A measured amount of the as-cast Al6061 is taken in the graphite crucible and agitated to a temperature of about 800 °C ± 5 °C in an electrical resistance furnace. Using hexa chloro ethane (C_2Cl_6) tablets, degasification is done to eject gases which engross in the melt during in situ reaction. Stochiometrically measured volumes of premixed halide salts of KBF_4 and Na_3AlF_6 (10 wt% of KBF_4) were agitated to 400 °C temperature in a muffle furnace to expel the dampness present in the salt and then poured into the melt. Continuous stirring was done with zirconia-coated stirrer and after reaction for an hour, at 800 °C temperature, the unwanted slag is removed from the melt and poured into a cast iron die preheated to a temperature of 300 °C. The fabricated castings of Al6061 alloy and prepared in situ AlB_2 composites were cleaned and machined according to ASTM standard for microstructural and corrosion characteristics. For the microstructural analysis, the specimens were metallographically cleaned and buffed with different grades of Silicon Carbide papers, followed by surface-finishing operation to 1 µm and finally by chemical incision with an acidic solution for disclosing microstructural characteristics [34–39]. Microstructures of the produced in situ composites were then analyzed using Scanning Electron Microscopy (SEM) for the structure of in situ AlB_2 dispersoids in the prepared composite.

The chemical reaction that takes place during the stirring of the melt is as follows [18]:

$$12KBF_4 + 13Al = AlB_{12} + 12KAlF_4 = AlB_{12} + 12KF + 12AlF_3 \quad (1)$$

$$2KBF_4 + 3Al = AlB_2 + 2KAlF_4 = AlB_2 + 2KF + 2AlF_3 \quad (2)$$

The exothermic chemical reactions that take place between (1) and (2) represent the explicit chemical processes which occur during the process of preparation and developing of in situ AlB_2 composites (Na_3AlF_6 can cause slags to eliminate aluminum oxide(Al_2O_3)).

$$2Al_2O_3 + 2\,Na_3AlF_6 = 4AlF_3 + Na_2Al_2O_4 + 2Na_2O \quad (3)$$

Table 1 Al6061 chemical compositions

Constituents	Fe	Si	Mn	Cu	Cr	Mg	Ti	Sn	Zn	Al
Percentage	0.31	0.42	0.135	0.234	0.24	0.84	0.269	0.001	0.24	Remainder

2.2 Corrosion Studies

Corrosion characteristics were studied using 3.5% sodium chloride with neutral pH which was made by liquefying 3.5 g of sodium chloride in 100 ml of water in a glass flask. Electrochemical measurements were done using three electrode cells. A platinum plate is used as a counter, while the reference electrode is made up of Ag/AgCl, and the prepared in situ composite is used as working electrode. Interface 1000 potentiostat/galvanostat controlled by a computer was used to obtain electrochemical measurements. Before the measurement, the working electrode was dipped into the solution containing sodium chloride for 60 min before a stable, free corrosion potential was recorded, while the temperature was maintained at 25 °C. The Tafel polarization curves were taken at a scanning rate of 0.01 V/s, quiet time of 2 s, and at the potentials ranging between − 1.788 and − 1.288 V versus platinum electrode. The corrosion characteristics of the composites were analyzed using corrosion potential Ecorr and anodic corrosion current density i_a.

3 Results and Discussions

3.1 Microstructural Studies

Figure 1a–c depicts the SEM micrographs of the as-cast and in situ Aluminum diboride MMCs. From Fig. 1a, it is observed that the SEM images of the as-cast Al6061 exhibit alpha-Aluminum dendrites, enveloped by an eutectic Silicon. Figure 1b shows the presence of AlB_2 particles in the matrix. According to Al–B phase diagram chart [40], AlB_2 is formed as per a peritectic-type chemical reaction of Al (liquid) + $AlB_{12} \rightarrow AlB_2$, during which, the AlB_{12} phase formed initially corresponds with the encompassing Aluminum melt to generate the in situ aluminum diboride particle with a slow cooling process. A vast majority of the Aluminum diboride particles produced in the in situ process have shown different shapes like hexagonal with light dim/gray dark shading as obviously observed in SEM images (Fig. 1b, c). As per the literature, shape of the boride particles was

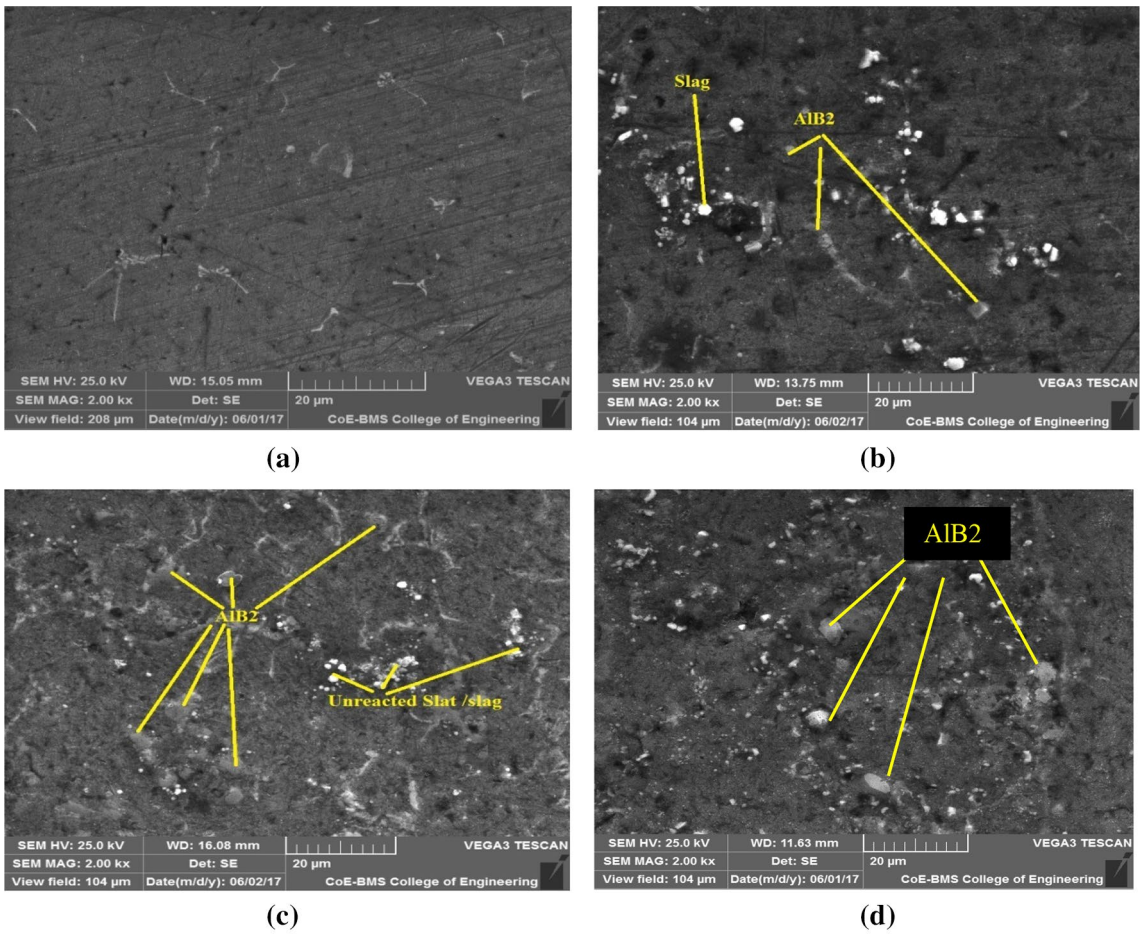

Fig. 1 **a**–**d** The SEM micrographs of Al6061 base matrix and AlB_2 in situ composites. **a** 6061Al Base matrix, **b** Al6061 + 1 wt% AlB_2, **c** Al6061 + 3 wt% AlB_2, **d** Al6061 + 5 wt% AlB_2 and clustering of particles

considered as hexagonal shape, hence the above result coincides with the literature [41]. Be that as it may, a couple of in situ AlB_2 particulates have different shapes namely spherical and elliptical. The in situ aluminum diboride particles generate better particles under nano scale because of which the nearness of huge single ceramic particles can be studied as group or cluster of particles [42]. A steady homogeneous distribution of in situ AlB_2 particles in the base Al6061 matrix can be accomplished by mixing the melt constantly which benefits in realizing the fracture of huge clustering of boride particles into tiny particles that can be consistently scattered in the base matrix. As seen in Fig. 1d, the agglomeration of the AlB_2 particles relies upon chemical reaction process, reaction temperature, response time, and cooling rate of the process. The characteristics of AlB_2 in situ composites exceptionally depend on the orientation, distribution, scattering, size, and shape of the reinforcement of Aluminum diboride particulates [43, 44].

3.2 Corrosion Studies

Figure 2a–d depicts the corroded SEM pictures of the as-cast alloy and in situ Al–AlB_2 MMCs. From the Fig.2 a–d, it is noticed that the composites are largely affected by pitting corrosion. Further, this phenomenon is influenced by AlB_2 content and its distribution in the composite. As the wt% of AlB_2 content increases, the corrosion rate reduces monotonically. The main reason for the corrosion rate of base matrix Al6061 and in situ AlB_2 composites in this particular case is due to the cracks and pits emerging on the specimen surface. The severity of corrosion is seen in cast alloy resulting in the formation of cracks on the surface. These cracks gradually develop into pits. Due to these cracks and pits, material has no resistance and is prone to suffer loss. Pits and cracks on the surface of the as-cast alloy are seen extensively because base alloy cannot produce any kind of resistance to the basic medium and base alloy is not provided

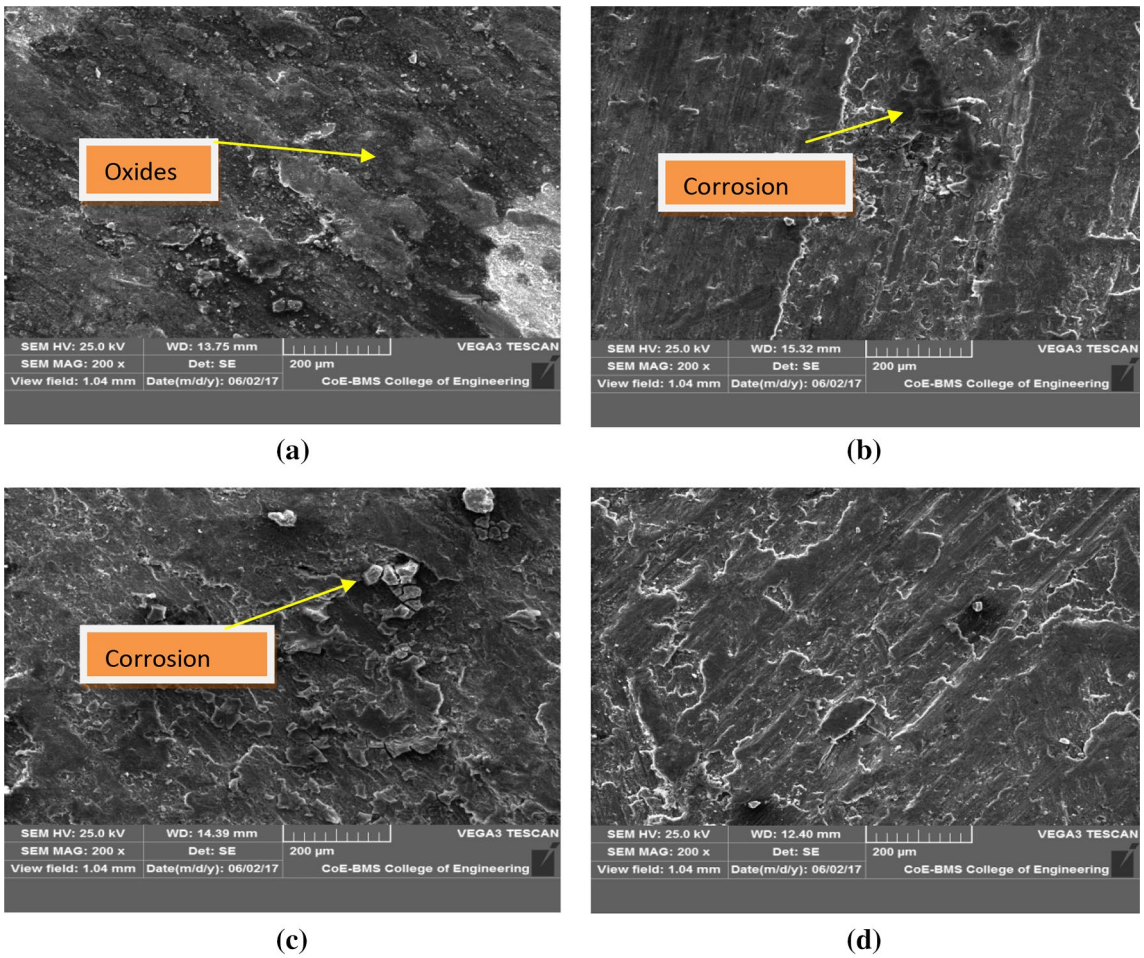

Fig. 2 **a–d** SEM micrographs of corroded specimens. **a** 6061Al base matrix, **b** Al6061 + 1 wt% AlB_2 particles, **c** Al6061 + 3 wt% AlB_2 particles, **d** Al6061 + 5 wt% AlB_2 particles

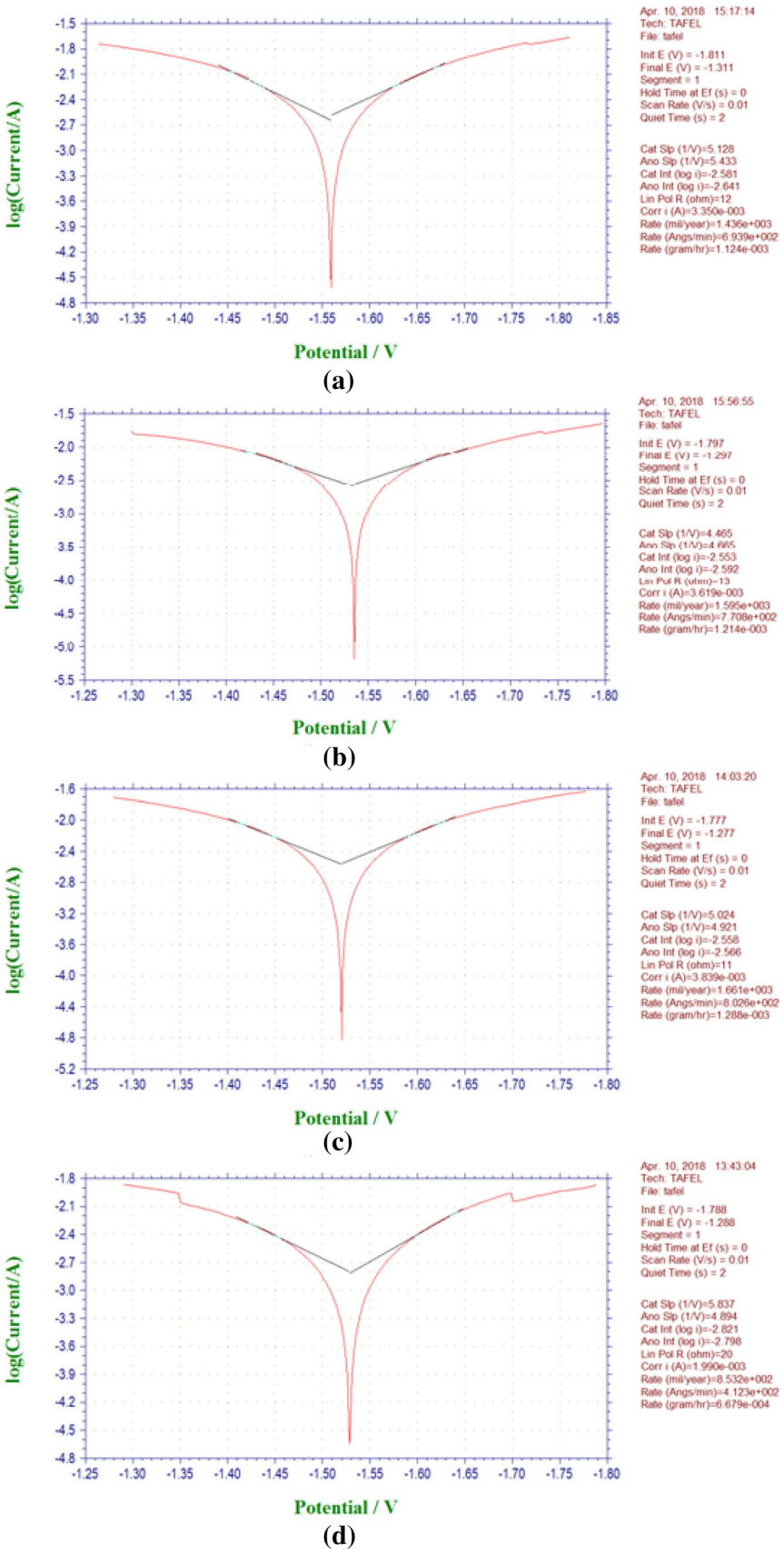

Fig. 3 **a**–**d** The Tafel plots for corrosion of **a** Al6061 base matrix, **b** Al6061 +1 wt% of AlB_2 particles, **c** Al6061 + 3 wt% of AlB_2 particles, **d** Al6061 + 5 wt% of AlB_2 particles

with reinforcement [45–48]. During corrosion, the disintegration of passive layer takes place by chloride ions since they penetrate via the layer of oxide. The polarization curve seemed to be shifting a little toward the current axis more than the base alloy with the increasing weight percentage of AlB_2 particulates. However, in acidic medium, the in situ AlB_2 particles behave as an insulator and remain inert [49]. Hence, with the increasing AlB_2 content in MMCs, the rate of corrosion falls, which leads to the abatement in the base matrix exposure area with the increasing reinforcement content. Corrosion and pitting are reduced when the composite surface is exposed to aggressive chlorine environmental process. Corrosion current density is reduced with the reinforcements in the MMCs, and it can be reduced further with the excessive reinforcement [25, 50]. More pits are seen on the matrix alloy than on MMCs.

3.3 Tafel Polarization Measurements

The effects of basic medium on the characteristics of corrosion of aluminum alloy and that of composite were examined at room temperature. The potentiostat polarization curves for the corrosion of matrix and composite material in NaCl medium are shown in Fig. 3a–d. The potential ranges between −T1.788 and − 1.288 V, which increases gradually with the increasing wt% of AlB_2 particles.

The potentiodynamic polarization in NaCl solution has helped in the analysis of the corrosion behavior of the composites. Both the anodic and cathodic curves of the polarization are similar for the corrosion behaviors of the composite with varying wt% of AlB_2 reinforcement in 3.5% NaCl solution. However, current density as well as corrosion potential of two composites was different [51]. From the graph, it is clear that increase in the potential signifies a clear decrease in the corrosion rate (Table 2). This indicates that, the rate of corrosion of the composites reduces with the increasing wt% of AlB_2 particles. The improvement in resistance to corrosion of Al matrix metal is due to the addition of AlB_2 reinforcement particles, which act as hard particles and also remain inert. Due to the increasing absorption of Chlorine ions onto the oxide layer or aluminum surface, the AlB_2 particles may breakdown due to stable oxide film present on the aluminum matrix. The improved rate of corrosion in the composites is because of the reinforcement particles altering the matrix microstructure and they act as physical guard to prevent the actuation and rate of progression for pitting corrosion [52]. The anodic polarization curves for the base alloy and composite show the continuity in corrosion current density indicating the susceptibility of pitting corrosion. This is assigned to the clean surface of Al6061 alloy reaching to the passivity rapidly when it is exposed to the oxygen-containing environment by forming the oxide film. The film adheres to the base metal surface, but since it contains flaws, pitting increases in chloride solution [53]. The boride particles, which are used as reinforcing elements, hamper the formation of oxide layer, and thereby diminish the rate of corrosion in the composite, significantly. The oxide layer causes formation of the protective barrier and lowers oxidation rate on the surface layer.

Table 2 The different compositions with corrosion potentials

Sl. no	Composition	Corrosion potential in mV
1	Al6061 Base matrix	− 1.56
2	Al6061 + 1 wt% of AlB_2	− 1.55
3	Al6061 + 3 wt% of AlB_2	− 1.53
4	Al6061 + 5 wt% of AlB_2	− 1.52

3.4 EDS and XRD

The EDS of the surface of the composite specimen indicates the presence of boron from the Al matrix. The presence of all the elements, viz., Si, Mg, Mn, Cr, Ti, Fe, and Cu in unreinforced Al alloy and the presence of K, F, and B from the halide salts in composites are shown in Fig. 4a. When the wt% of AlB_2 reinforcement increases, the atomic weight of the composite increases as shown in Fig. 4b–d. This indicates the halide salt mixed thoroughly in the melt.

XRD analysis was conducted to verify the completion of reaction, and the results are shown in Fig. 5a for AA6061/AlB_2 composites with different compositions of 3 and 5 wt% of AlB_2 particles. The diffraction of AlB_2 peaks appearing in the XRD pattern confirms the formation of AlB_2. It is also observed that the intensity of AlB_2 peaks increases with the increasing wt% of AlB_2 particles.

4 Conclusions

Following conclusions were made on the in situ-developed AlB_2 MMCs, produced by the exothermic chemical reaction between Al6061 matrix alloy and KBF_4 halide salt.

1. The in situ composites were successfully fabricated with 1, 3, and 5 wt% of AlB_2 particles in Al6061 base matrix in a resistance furnace using stir casting.
2. SEM micrographs reveal clean and clear in situ AlB_2 particles, distributed uniformly throughout the base matrix with less agglomeration.
3. The rate of corrosion for Al6061 base matrix is higher than that of the in situ composite produced. The Tafel plots show higher rate of corrosion in Al6061 alloy com-

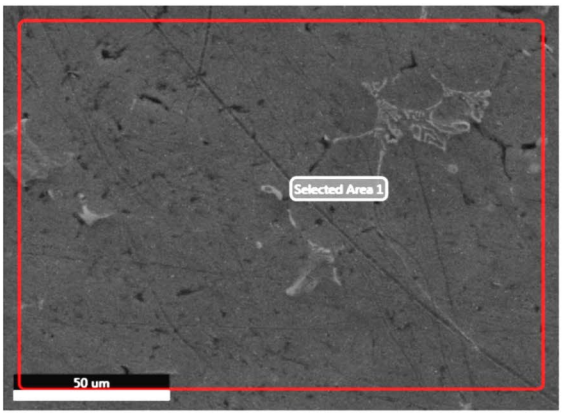

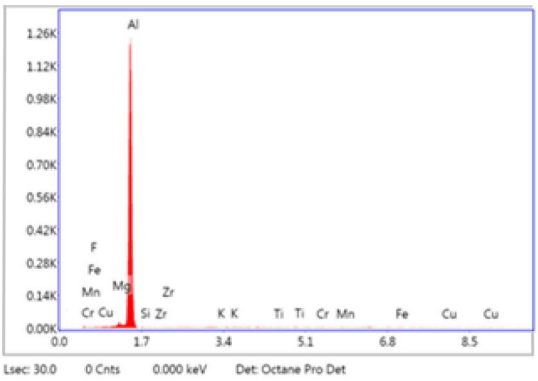

Element	Weight %	Atomic %
F K	0.02	0.02
MgK	1.75	1.75
AlK	85.17	76.89
SiK	8.90	19.46
ZrL	0.17	0.05
K K	0.49	0.30
TiK	0.42	0.22
CrK	0.51	0.24
MnK	0.46	0.20
FeK	1.00	0.44
CuK	1.11	0.43

(a)

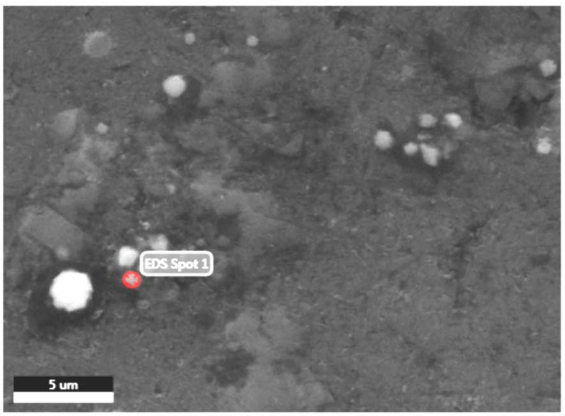

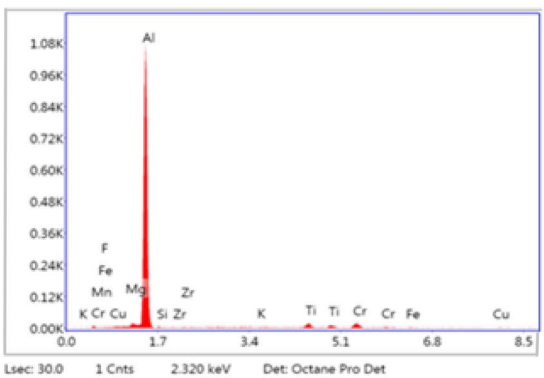

Element	Weight %	Atomic %
B K	16.41	34.11
F K	0.02	0.03
MgK	1.21	1.12
AlK	72.10	60.04
SiK	0.65	0.52
ZrL	0.26	0.06
K K	0.45	0.26
TiK	2.89	1.36
CrK	4.34	1.88
MnK	0.52	0.21
FeK	0.43	0.17
CuK	0.73	0.26

(b)

Fig. 4 **a**–**d** The EDS images of **a** Al6061, **b** Al6061 + 1 wt% of AlB_2, **c** Al6061 + 3 wt% of AlB_2, **d** Al6061 + 5 wt% of AlB_2

Fig. 4 (continued)

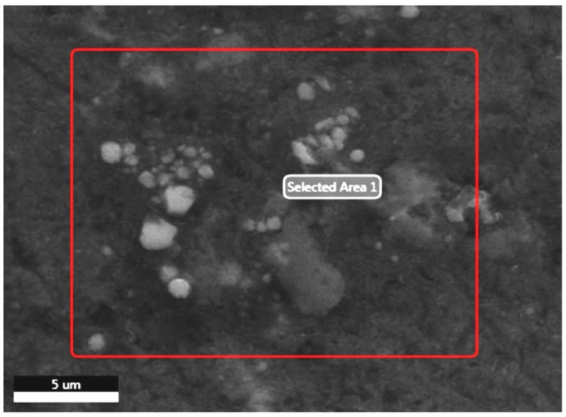

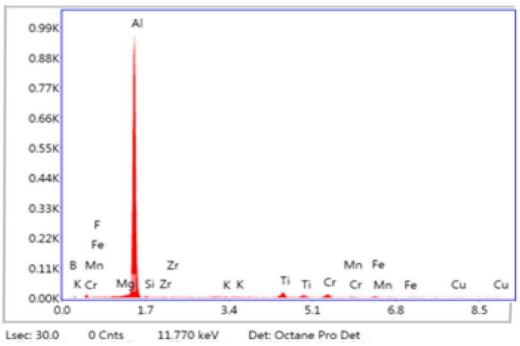

Element	Weight %	Atomic %
B K	20.47	40.70
F K	0.02	0.03
MgK	0.61	0.54
AlK	67.27	53.61
SiK	0.92	0.70
ZrL	0.51	0.12
K K	0.62	0.34
TiK	3.55	1.59
CrK	3.14	1.30
MnK	0.56	0.22
FeK	1.28	0.49
CuK	1.05	0.36

(c)

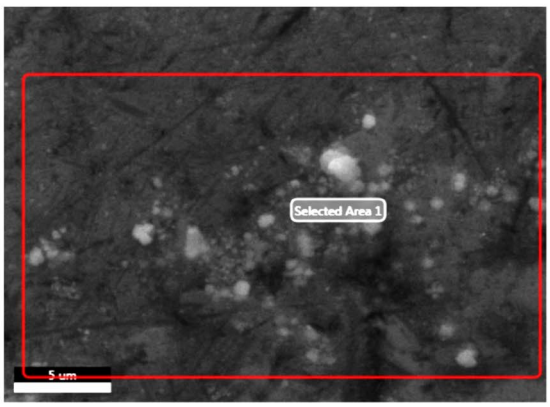

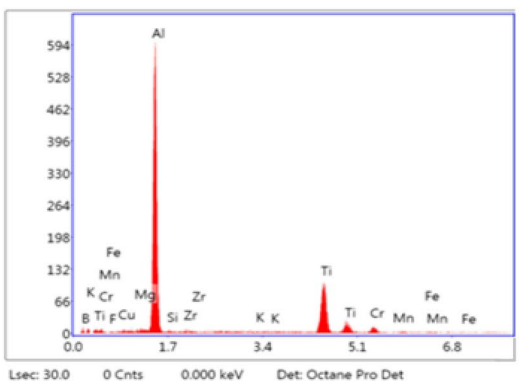

Element	Weight %	Atomic %
B K	52.70	76.74
F K	0.15	0.13
MgK	0.47	0.30
AlK	29.89	17.44
SiK	0.25	0.14
ZrL	0.45	0.08
K K	0.24	0.10
TiK	12.51	4.11
CrK	2.07	0.63
MnK	0.28	0.08
FeK	0.43	0.12
CuK	0.55	0.14

(d)

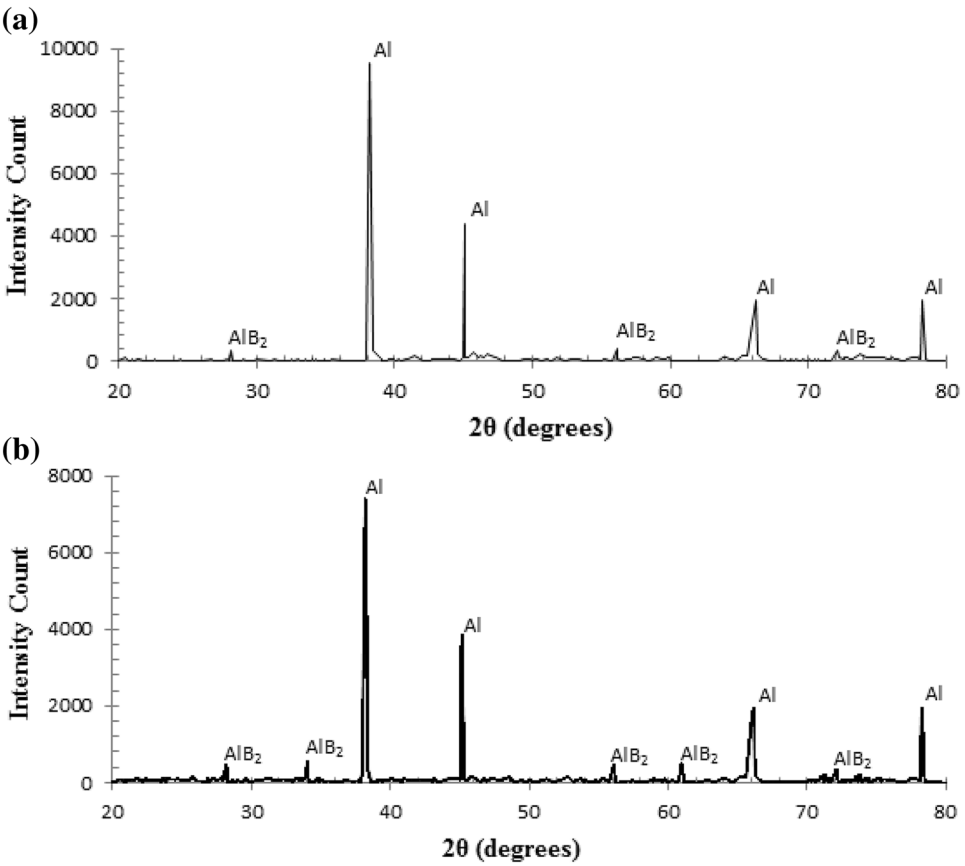

Fig. 5 **a**, **b** The XRD images of **a** Al6061 + 3 wt% of AlB_2, **b** Al6061 + 5 wt% of AlB_2

pared to 5 wt% of AlB_2 in situ composites. This predicts that with the percentage increase of reinforcement, the rate of corrosion rate reduces significantly.

4. Normality of NaCl plays an important role in corrosion process in the deflection of polarization curves. The corrosion rates of the base matrix and in situ composites directly depend on the concentration of NaCl.

Acknowledgements The authors wish to express their profound sense of gratitude to the East West Institute of Technology, Bengaluru for the support and facility provided to carry out the corrosion studies.

References

1. Ghomashchi MR, Vikhrov A (2000) Squeeze casting: an overview. J Mater Process Technol 101:1–9
2. Dayanand Samuel, Satish Babu B, Auradi V (2018) Experimental investigation on micro structural and dry sliding wear behavior of Al-AlB_2 metal matrix composites. Material Today 5:22536–22542
3. Murthy BS, Kori SA, Venkateshvaralu K, Bhat RR, Charoborthy M (1999) Manufacture of Al-Ti-B master alloy by the reaction of complex halide salt with molten aluminium. J Mater Proces Technol 89:152–158
4. Uju WA, Oguocha INA (2009) Thermal cycling behaviour of stir cast Al-Mg alloy reinforced with fly ash. Mater Sci Eng, A 526:100–105
5. Seah KHW, Hemanth J, Sharma SC (2003) Mechanical properties of aluminum quartz particulate composites cast using metallic and non-metallic chills. Mater Des 24:1987–1993
6. Ramesh CS, Anwar Khan AR, Ravikumar N, Savanprabhu P (2005) Prediction of wear coefficient of Al6061-TiO_2 composites. Wear 259:602–608
7. Ashok Kumar B, Murugan N (2012) Metallurgical and mechanical characterization of stir cast AA6061-T6-AlNp composite. Mater Des 40:52–58
8. Ramesh CS, Keshavamurthy R (2011) Slurry erosive wear behavior of Ni-P coated Si_3N_4 reinforced Al6061 composites. Mater Des 32:1833–1843
9. Gopalakrishnan S, Murugan N (2011) Prediction of tensile strength of friction stir welded aluminum matrix TiCp particulate reinforced composite. Mater Des 32:462–467
10. Kalaiselvan K, Murugan N, Parameswaran S (2011) Production and characterization of AA6061-B_4C stir cast composite. Mater Des 32:4004–4009
11. Vijay SJ, Murugan N (2010) Influence of tool pin profile on the metallurgical and mechanical properties of friction stir welded Al–10 wt% TiB_2 metal matrix composite. Mater Des 31:3585–3589
12. Naveen Kumar G, Narayanasamy R, Natarajan S, Kumaresh Babu SP, Sivaprasad K, Sivasankaran S (2010) Dry sliding wear behaviour of AA 6351-ZrB_2 in situ composite at room temperature. Mater Des 31:1526–1532
13. Feng CF, Froyen L (2000) Microstructures of in situ Al/TiB_2 MMCs prepared by a casting route. J Mater Sci 35:837–850
14. Birol Yucel (2009) Production of Al-B alloy by heating Al/KBF_4 powder blends. J Alloys Compds 481:195–198

15. Boppanna S, Channakeshavalu K (2009) Preparation of Al-TiC metal matrix composites. J Miner Mater Charact Eng 8(6):563–568
16. Wang X (2005) The formation of AlB_2 in an Al- B master alloy. J Alloys Compd. 403:283–287
17. Kayikcia R, Savas O, Koksala S, Demira A (2014) The effect reinforcement ratio on the wear behaviour of AlB_2 flake reinforced metal matrix composites. Acta phycica Polonic A 125(2)
18. Draguţ DV, Uşurelu E (2011) Characterization of in situ AA 6060/AlB_2 metal matrix composite. U.P.B. Sci Bull. Ser B 73
19. Orbán R, Cora I, Dódony I (2012) Preparation and characterization of an aluminum/aluminum diboride composite. In: ECCM15-15th European conference on composite materials, Venice, Italy, 24–28 June 2012
20. Kubota M (2004) Properties of Al-AlB_2 materials processed by mechanical alloying and spark plasma sintering proceedings. In: 9th international conference on aluminium alloys (2004) Edited by J.F. Nie, A.J. Morton and B.C. Muddle Institute of Materials Engineering Australasia Ltd
21. Prasad KVS, Murthy BS, Pramanik P, Mukunda PG, Chakramurthy M (1996) Reaction fluorides salts with aluminuim. Mater Sci Technol 12:766–770
22. Koksal S, Ficici F, Kayikci R, Savas O (2012) Experimental investigation of dry sliding wear behaviour of insitu AlB_2/Al composite based on taguchi's method. Mater Des 42:124–230
23. Maldovan P, Dragut DV (2015) In-situ productions of Al/AlB_2 composite by metal salt reaction, www.researchgate.net.publication. https://doi.org/10.13140/rg2.1.1339.5367. May 2015
24. Huda MD, Hashmi MS, El-Baradie MA (1995) MMCs: materials, manufacturing and mechanical properties. In: Key engineering materials, vol 104. Trans Tech Publications, pp. 37–64)
25. Sherif ESM, Almajid AA, Latif FH, Junaedi H (2011) Effects of graphite on the corrosion behavior of aluminum-graphite composite in sodium chloride solutions. Int J Electrochem Sci 6:1085–1099
26. Abdul-Jameel HP, Nagaswararpa P, Krupakara V, ShashiShekar TR (2009) Evaluation of corrosion rate of Al 6061-Zirconia metal matrix composites in sea water. Int J Ocean Oceanogr 3(1):37–42
27. Alaneme KK, Bodunrin MO (2011) Corrosion behavior of alumina reinforced metal matrix composites. JMMCE 10(12):1153–1165
28. Achutha Kini U, Shetty Prakash, Divakara Shetty S, Arun Isloor M (2011) Corrosion inhibition of 6061 aluminum alloy/SiC composite in HCl acid medium using 3-Chloro-I-Benzothiophene-2-carbohydrazide. Indian J Chem Technol 18:439–445
29. Seah KHW, Krishna M, Vijayalakshmi VT, Uchil J (2002) Corrosion behavior of garnet particulate reinforced LM 13 alloy MMCs. Corros Sci 44:917–925
30. Zuhair GM, Al-qutub AM (2002) Corrosion behavior of powder metallurgy aluminum alloy 6061/Al_2O_3 metal matrix composites. In: The 6th Saudi Engg conference, vol 5, pp 271–281
31. Pruthviraj RD, Krupakara PV, Parashuram BS (2006) Effect of reinforcement content on the corrosion properties of aluminium 7075/SiC composites in equimolar solution of sodium hydroxide and sodium chloride solution. Bull Electrochem 22(6):281–284
32. Krupakara PV (2013) Corrosion characterization of Al6061/red mud metal matrix composites. Portugaliae Electro chimica Acta 31(3):157–164
33. Auradi V, Kori SA (2008) Influence of reaction temperature for the manufacturing of Al-3Ti and Al-3B master alloys. J Alloys Compds 453:147–156
34. Tjong SC, Wang GS, Geng L, Mai YW (2004) Cyclic deformation behaviour of insitu aluminium matrix composite of the system Al-Al_3Ti-TiB_2-Al_2O_3. Compos Sci Technol 64:1971–1980
35. Karantzails AE, Lekatou A, Gerogties M, Poulas V, Mavros H (2011) Casting based production of Al-TiC-AlB_2 composite material through the use of KBF_4 salt. J Mater Eng Perform 20(2):198–202
36. Ficici F, Koksal S, Kayikci R, Savas O (2011) Investigation of unlubricated sliding wear behaviours of in situ AlB2/Al metal matrix composite. Adv Compos Lett 20(4):096369351102000404
37. Savaş Omar, Koksal Sakip, Kayikci Ramazan (2012) Application of taguchi method to investigate the effect of some factors on in situ formed flake structures of Al/AlB_2 composite. Adv Compos Lett 21(2):49
38. Draught DV, Maldovan P, Butu M, Usurelu E (2011) Characterization of in situ AA6060/AlB_2 metal matrix composite. UPB Sci Bull Ser B 73:4
39. Mirkovic D, Irkovic D, Grobner J, Schmid-Fetzer R, Fabrichnaya O, Lukas HL (2004) Experimental study and thermodynamic reassessment of the Al-B system. J Alloys Compds 384:168–174
40. Kayikcia R, Sava B, Koksala S, Demira A (2013) The effect of reinforcement ratio on the wear behaviour of AlB_2 flake reinforced MMCS. In: Proceedings of the 3rd international congress apmas, April 24–28: Antalya, Turkey
41. Jackson MJ, Graham ID (1994) Mechanical stirring of Al-B alloys. J Mater Sci Lett 13:754–756
42. Tjong SC, Ma ZY (2000) Microstructural and mechanical characteristics of in situ metal matrix composites. Mater Sci Eng, R 29:49–113
43. Xiao-ming W (2005) The formation of AlB_2 in an Al-B master alloy. J Alloys Compds 403:283–287
44. Wang QL, Zhao HS, Li ZG, Shen L, Zhao JZ (2013) Production of Al-B master alloys by mixing KBF_4 salt into molten aluminum Trans. Nonferrous Met Soc China 23:294–300
45. Elicicek H, Savas O, Ayadin Z, Ozdemir O K, Kayaki R (2016) Corrosion behavior of in situ AlB_2/Al-Cu metal matrix composites. Acta Physica polonica A 129(4)
46. Shanbhag VV, Yalamoori NN, Yalamoori S, Kartikeyan S, Ramanujam R (2014) Fabrication surface morphology and corrosion investigation of Al7075-Al_2O_3 matrix composites in sea water and industrial environment. Proceedia Eng 97:607–613
47. Bienias J, Walczak M, Surowska B, Sobczak J (2003) Microstructure and corrosion behavior of aluminum fly ash composites. J Optoelectron Adv Mater 5(2):493–502
48. Anandmurthy HC, Singh SK (2015) Influence of TiC particulate reinforcement on the corrosion behavior of Al6061 metal matrix composites. Adv Mater Lett 6(7):633–640
49. Abbass MK, Hassan KS, Alwan AS (2015) Study of corrosion resistance of aluminum alloy 6061/SiC composites in 35% NaCl solution. Int J Mater Mech Manuf 3(1):31–35
50. Chunlin HE, Changsheng LIU, Li Fengquin (2002) Corrosion behavior and protection efficiency of 2024 Al and SiCp/2024Al metal matrix composites. J Mater Sci Tecnol 18(4):351–353
51. Ashok SD, Mamatha GP, Venkatesh TV, Pruthvaraj RD (2015) Corrosion characterization of aluminum 7075/silicon carbide metal matrix composite. Int J Adv Res Chem Sci 2(1):24–29
52. Ramchandra M, Dilip Kumar G, Rashmi R (2016) Evaluation of corrosion property of aluminum zirconium dioxide (Al-ZrO_2) nano composites. Int J Chem Mol Nucl Mater Metall Eng 10(10):1321–1326
53. Han YM, Chen X (2015) Electrochemical behavior of Al-B4C metal matrix composites in NaCl solution. Materials 8(9):6455–6470